



---

# Charge Dynamics in Vegetable Oil-Based Ester Dielectric Fluid

A. A. Abdelmalik<sup>1\*</sup>

<sup>1</sup>*Department of Physics, Ahmadu Bello University, Zaria, Nigeria.*

### **Author's contribution**

*This work was carried out by author. He designed the study, performed the test and analysis. The author read and approved the final manuscript.*

**Original Research Article**

**Received 8<sup>th</sup> March 2013**  
**Accepted 17<sup>th</sup> May 2013**  
**Published 19<sup>th</sup> October 2013**

---

## ABSTRACT

Alkyl ester derivatives of palm kernel oil have been prepared for use as bio-dielectrics in oil filled HV electric equipment. Conduction and loss characteristics of the ester derivatives were studied to understand the behaviour of the material under electric field. Frequency response analyzer was used to study electrical conduction within the fluids since dielectric loss occurring at low frequencies under AC condition is dominated by mobile charge carriers. This is particularly important since power dissipation at power frequency, 50 Hz, may lead to dielectric heating. The dielectric response analysis of the samples with the range  $10^{-3}$  -  $10^4$  Hz show a constant real relative permittivity at high frequency region. As the frequency drops below  $10^1$  Hz, there is interfacial polarization at the electrode-liquid interface, which results in a significant dielectric increment in the real part of the relative permittivity at low frequencies with a negative slope greater than 1 and a frequency independent conductance ( $\epsilon'$  slope = -1). This is an indication of Maxwell-Wagner interfacial effect where electric double layer (EDL) is formed. The real part acquired a slope of about -1 around frequency of  $10^3$  Hz. This suggests that the establishment of the EDL may be tending towards steady state. This change in the low frequency dispersion could be due to the ionic species undergoing interfacial electrochemical processes, or ions of lower mobility may have contributed to the EDL formation within the frequency region. This may have limited the effect of the strongly divergent processes at the interface.

---

\*Corresponding author: E-mail: [aaabdelmalik@abu.edu.ng](mailto:aaabdelmalik@abu.edu.ng);

*Keywords: Charge transport; dielectric loss; electric double layer; dielectric liquid; frequency dispersion.*

## 1. INTRODUCTION

An understanding of the dielectric behaviour of insulating liquid requires the study of the dielectric response over a spectrum of frequency covering several decades and temperatures. Interfacial polarization is known to dominate measurements at low frequencies (frequency below  $10^{-1}$  Hz); as a result such measurement may reveal useful information about the charged particles in the liquid and their behaviour [1]. Since dielectric loss occurring at low frequencies under AC conduction is dominated by mobile charge carriers, the study of AC conduction within an insulating fluid is particularly important since power dissipation at power frequency, 50 Hz, may lead to dielectric heating.

For a nearly perfect dielectric material, application of a sufficiently low alternative field produces no detectable phase difference ( $\delta$ ) between the voltage gradient ( $\bar{E}$ ) and displacement vector ( $\bar{D}$ ). The ratio of the two vectors gives a real value constant referred to as the permittivity. An ideal dielectric material has finite dielectric loss and in simple terms can be said to behave like parallel RC circuit (Fig. 1). The values of R and C may be frequency dependent and the relative permittivity of the material becomes a complex quantity. The resistance R represents the lossy part of the dielectric which may result from electronic and/or ionic conductivity, dipole orientation, and space charge accumulation on the application of electric field. The storage capacity of the dielectric may be visualized as the action of dipole chains which forms under the influence of the applied field and bind counter-charges with their free ends on the surfaces of the plates [2].

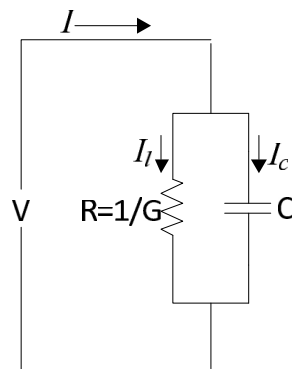


**Fig. 1. Parallel equivalent circuit of a dielectric**

For a pure DC conduction in condensed matter, the real part of the relative permittivity,  $\epsilon'$ , is close to zero and independent of frequency. Acquisition of slope by  $\epsilon'$  at low frequency in the log-log plot of real part, is due to polarizing species that is dominated by slowly mobile charge carriers and the slope of the imaginary part,  $\epsilon''$ , with an approximate value of -1 in a log-log plot of the imaginary part,  $\epsilon''$  vs  $\omega$ , is an indication of a low frequency dispersion (LFD). Low frequency dispersion can be volume or interfacial processes. While the presence of interfacial barrier layer at the electrode-sample interface is sometimes referred to as

interfacial LFD, volume LFD is distributed throughout the thickness of the material. The loss in the material in this case is more than just a mere DC conduction. This type of response seems to be the lowest-frequency process observed in frequency response of dielectric material and has been termed the anomalous low-frequency dispersion (LFD) [3]. The strong rise of  $\epsilon'$  at low frequencies has a physical significance which indicates a finite and reversible storage of charge in the bulk material or at the material-electrode interface [4]. The curves of  $\epsilon'$  and  $\epsilon''$  cross over at  $\omega_c$ , the threshold frequency as shown in Fig. 2. At a frequency below the threshold frequency,  $\omega_c$ , ( $\omega < \omega_c$ ), this response follows a fractional power law which is expressed as:

$$\epsilon^*(\omega) = A(i\omega)^{n_2-1} = A[\sin(n_2\pi/2) - i \cos(n_2\pi/2)]\omega^{n_2-1} \tag{1}$$

In this low frequency region  $\epsilon'' > \epsilon'$ , the frequency response is due to highly lossy “drift like” processes. The high frequency response, ( $\omega > \omega_c$ ) may follow a similar power law but with the exponent equal to  $n_1$  as expressed below. This is due to a low-loss “polarization like” process.

$$\epsilon^*(\omega) = A(i\omega)^{n_1-1} = A[\sin(n_1\pi/2) - i \cos(n_1\pi/2)]\omega^{n_1-1} \tag{2}$$

Where constant  $A$  is an empirical constant and  $n_1$  and  $n_2$  have value between 0 and 1 [5].

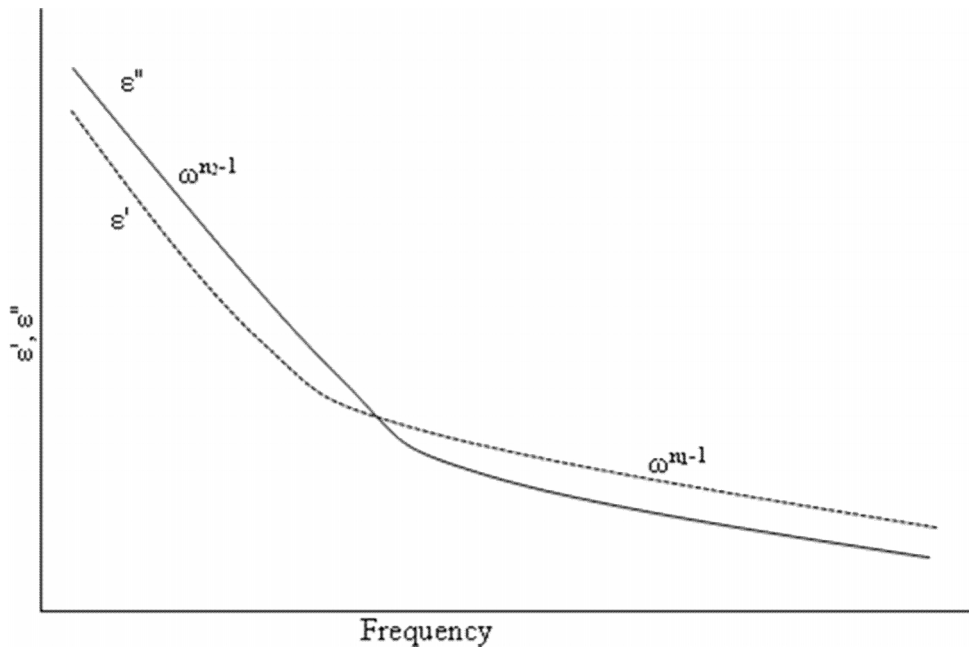


Fig. 2. Low frequency dispersion (LFD) process [4]

This paper concentrates on the study of conduction and loss characteristics of the ester derivatives using dielectric spectroscopy with a focus on low temperature and low frequency response. This is mainly to establish the dielectric behaviour of the material under electric field and the influence of processing steps on the ester derivatives at varied frequencies. It is

known that during oil synthesis, remnant of some chemicals used for the ester synthesis were present in the ester sample. They remnants may undergo electrochemical processes and could constitute impurities in the samples. Dielectric spectroscopy, in which the complex impedance is measured over a wide range of frequencies, is known to be highly sensitive to small changes in electrical properties. It was thought that dielectric spectroscopy would provide a means of identifying the influence of synthesis steps in the dielectric properties of the ester derivatives. Using dielectric spectroscopy it would be possible to establish whether the impurities present in the samples could result in the dissipation of too much power, causing overheating and premature failure of the ester fluids if used as dielectric fluids.

## 2. MATERIALS AND METHODS

### 2.1 Sample Preparation

An alkyl ester (PKOAE1) was synthesized from laboratory purified palm kernel oil by transesterification. Epoxy alkyl ester (PKOAE2) was then synthesized by epoxidation of PKOAE1 with an insitu peracetic acid [6]. Branched alkyl esters (PKOAE3 and PKOAE4) were then prepared using an acid-catalyzed ring-opening reaction of PKOAE2 and acid anhydrides in the presence of nitrogen [7]. Sample descriptions are summarized in Table 1. The samples were dried by degassing at reduced pressure in a vacuum oven at temperature of 85°C for 2 hours.

**Table 1. Sample description**

Sample	Description
PKOAE1	Palm kernel oil methyl ester
PKOAE2	Palm kernel oil epoxy methyl ester
PKOAE3	Palm kernel oil methyl ester with C-3 carbon side branched chain
PKOAE4	Palm kernel oil methyl ester with C-4 carbon side branched chain
BS148	Mineral Insulating Oil

### 2.2 Structural Identification

Natural ester consists of fatty acids of various chain lengths. The synthesis involves a change in the chemical structure through modification of some of the fatty acids' chains in the ester. It is necessary to monitor the chemical reaction to know if the required products are obtained and identify the functional groups in the synthesized esters. This was achieved using Fourier Transform Infrared (FT-IR) Spectrometry. This analysis was performed using Perkin Elmer Spectrum One FT-IR spectrometer. The spectrometer sample holder and the cap were cleaned with methanol and acetone thoroughly. The cap was fixed and a background scan was performed. A drop of the sample was placed on the spectrometer measurement cell. The sample was scanned with infrared radiation through frequency of 4000 - 650  $\text{cm}^{-1}$  to obtain the spectrum. The amount of radiation absorbed by the sample was plotted as a function of the wave number of the absorbed radiation by a detector. Each spike (absorption bands) in the IR spectrum represents absorption of energy. The functional groups of the samples were identified from the spectra.

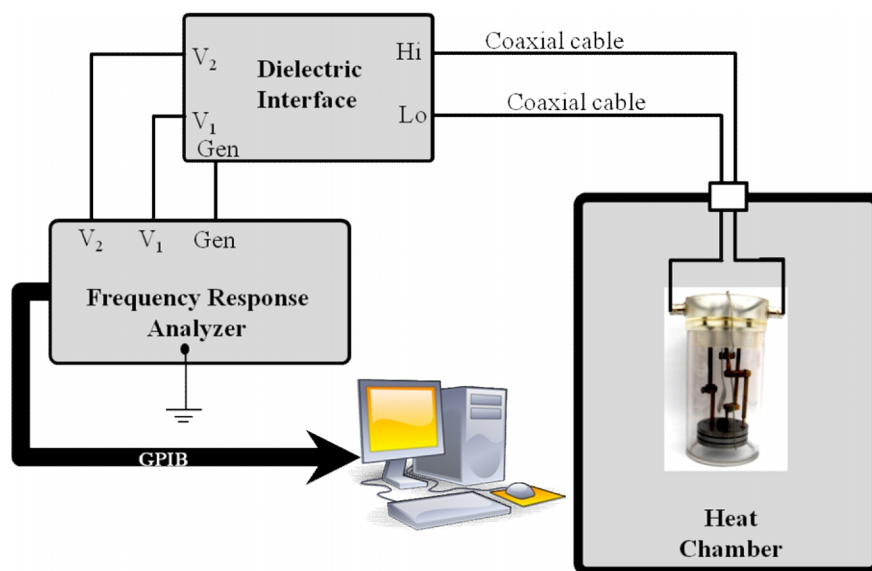


Fig. 3. FRA experimental system for dielectric liquid

### 2.3 Dielectric Response Measurements

The dielectric properties of the samples were measured in a bespoke test cell designed such that the electrodes were suspended in the oil sample and had enough space to accommodate sample expansion [8]. The dielectric response of the samples was measured using a Solartron 1255 Frequency Response Analyzer and 1296 Dielectric Interface as shown in Fig. 3. Dielectric measurements were taken over the frequency range  $10^{-3}$  Hz to  $10^6$  Hz and at number of fixed temperatures within the range  $20^{\circ}\text{C}$  to  $80^{\circ}\text{C}$ . The temperature of the sample was varied to within  $0.1^{\circ}\text{C}$  by placing the cell in a temperature-controlled oven.

## 3. RESULTS AND DISCUSSION

### 3.1 Structural Study

The FTIR spectra (Figs. 4 and 5) displayed the characteristic peak of some functional groups common to the ester samples. PKOAE2 exhibits peaks around  $844\text{ cm}^{-1}$  [9] due to the presence of epoxy group in the palm kernel oil alkyl ester. These peaks are characteristic of ester that has been epoxidized. These can be regarded as fingerprint of epoxy alkyl ester as the peaks fall within the fingerprint region. The existence of the peaks at  $844\text{ cm}^{-1}$  on the PKOAE2 spectra shows that the transesterification reaction occurred without degradation of the epoxy ring, which is needed for further modification of epoxy alkyl ester.

The reaction of the ester with butyric anhydride (PKOAE3) yields a FTIR peak at  $1080\text{ cm}^{-1}$  as shown in Fig. 5, which is attributed to a grafted C-3 side branched hydrocarbon chain. If instead propionic anhydride is reacted with the ester, the grafted C-4 side branched hydrocarbon chain (PKOAE4) has a peak at  $930\text{ cm}^{-1}$ . These peaks can be considered as fingerprints of the respective esters: they uniquely differentiate the two alkyl esters. These peaks fall within the fingerprint region of FTIR spectra. These could be attributed to the

fingerprint of the respective esters. The peaks are unique to the respective esters and they differentiate the two alkyl esters.

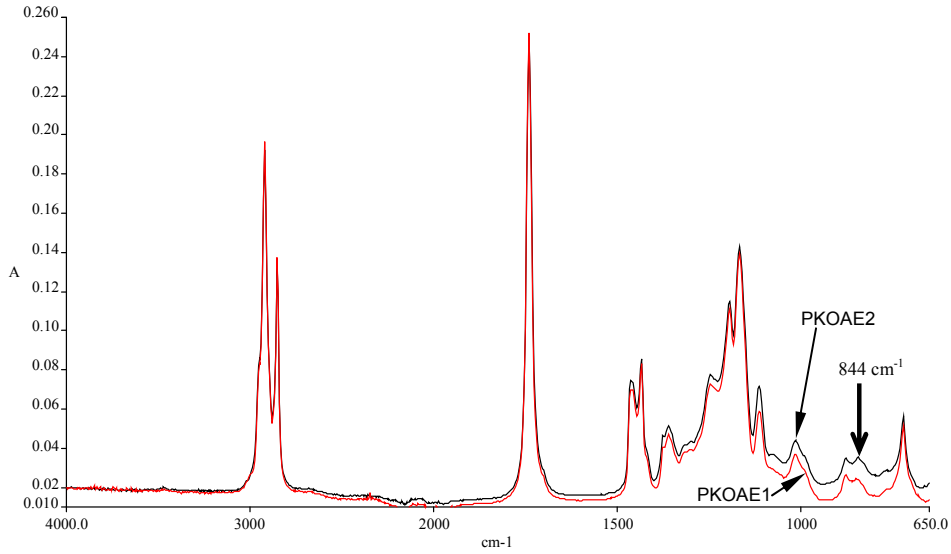


Fig. 4. FTIR spectra of PKOAE1 and PKOAE2

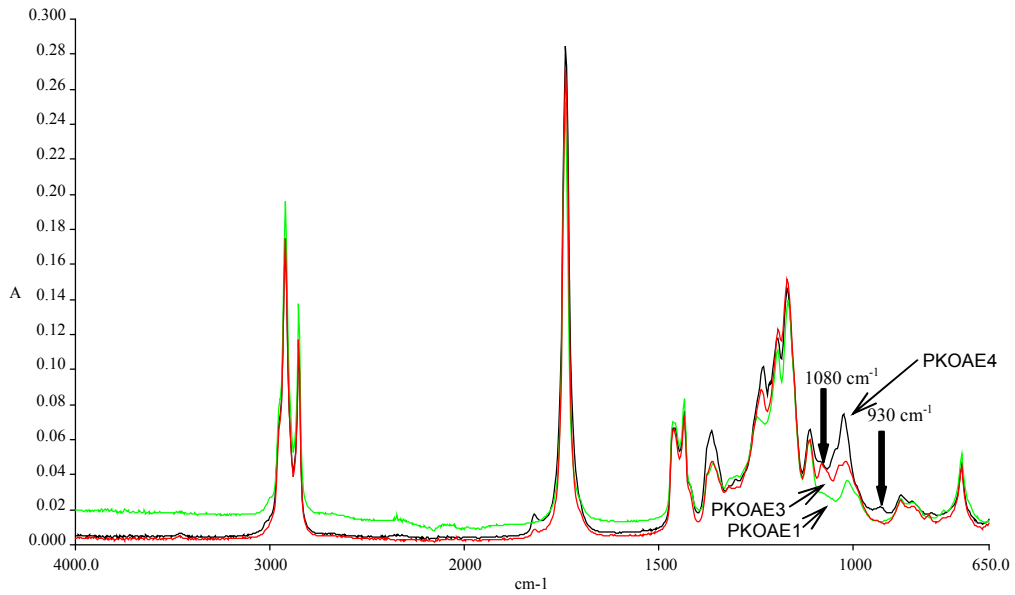


Fig. 5. FTIR spectra of PKOAE1, PKOAE3 and PKOAE4

### 3.2 Frequency Response Analysis

Previous study on the palm kernel oil-based ester fluid shows that it has suitable properties as alternative bio-based insulating fluid. The ester derivative possessed a flash point that

satisfied the specified minimum flash point for mineral oil, higher thermo-oxidative stability, and high and reliable breakdown strength from the distribution of breakdown data (43 kV/mm) with melting temperature of about -7°C [6,8]. Dielectric response of samples of PKOAE1, PKOAE2, PKOAE3 and PKOAE4 were measured. The dielectric response of the synthesized esters above the frequency of approximately  $10^{-2}$  Hz shows that the real part is constant (i.e. independent of frequency) and the imaginary part is inversely proportional to frequency. This is symptomatic of a constant capacitance in parallel with a constant conductance – that is, a constant electrical conduction mechanism dominates in this frequency range. At lower frequencies, the real part acquires a negative slope greater than 1 at  $10^{-2}$  Hz whilst the imaginary part still maintains a slope of -1. This is indicative of interfacial polarization [10] with a more complex low frequency response. Temperature variations often influenced the response of dielectric material on the application of electric field. This change in temperature may lead to variation in the individual relaxation times. This will result in a shift of the respective  $\tan\delta$  peak along the logarithmic frequency axis. The effect of temperature on the characteristic frequency of the materials can be studied with a single curve known as master curve. This curve is constructed by normalizing the data for different temperatures. This is done by shifting the spectra for different temperatures into coincidence. If there is more than one process, e.g. a DC conduction and an (AC) polarization processes, and if this processes have different dependencies on temperature, then it will only be possible to bring the part of spectra corresponding to one process into coincidence using this process. A logarithmic shift was performed on the response of the samples along the frequency axis by using DC conduction to bring the spectra into coincidence. The spectrum at 20°C was chosen as the reference while the spectra at other temperatures were shifted towards it. The magnitude was invariant and as a result, the logarithmic shift along the frequency axis was carried out with the relation:

$$\text{shift factor} = \log a_T = \log(\omega_i) - \log(\omega_{ref}) = \frac{E_a}{k} \left( \frac{1}{T_{ref}} - \frac{1}{T_i} \right) \quad (3)$$

Where  $\log a_T$  is the logarithmic shift between any two frequencies,  $\omega_{ref}$  and  $\omega_i$  along the frequency axis corresponding to the same magnitude of the dielectric response function at  $T_{ref}$  and  $T_i$ .  $E_a$  is the activation energy.

Both real and imaginary parts are inter-dependent from Kramer Kronig relation; as a result equation (3) was applied to both the real and imaginary part of the relative permittivity [10]. The dielectric spectra at 20°C were made the reference spectra and the spectra at higher temperatures were shifted to match the reference spectra to form the master curve. The obtained master plots of the real and imaginary components of the relative permittivity as a function of frequency (i.e. a Bode plot) of the alkyl esters of palm kernel oil are shown in Fig. 6 through Fig. 9. The frequency response displayed a departure from simple Debye type relaxation. The real part is constant (i.e. independent of frequency) above approximately  $10^{-1}$  Hz, while the imaginary part is inversely proportional to frequency with a slope of -1. This behaviour is an indication of a conduction mechanism dominating in this frequency range.

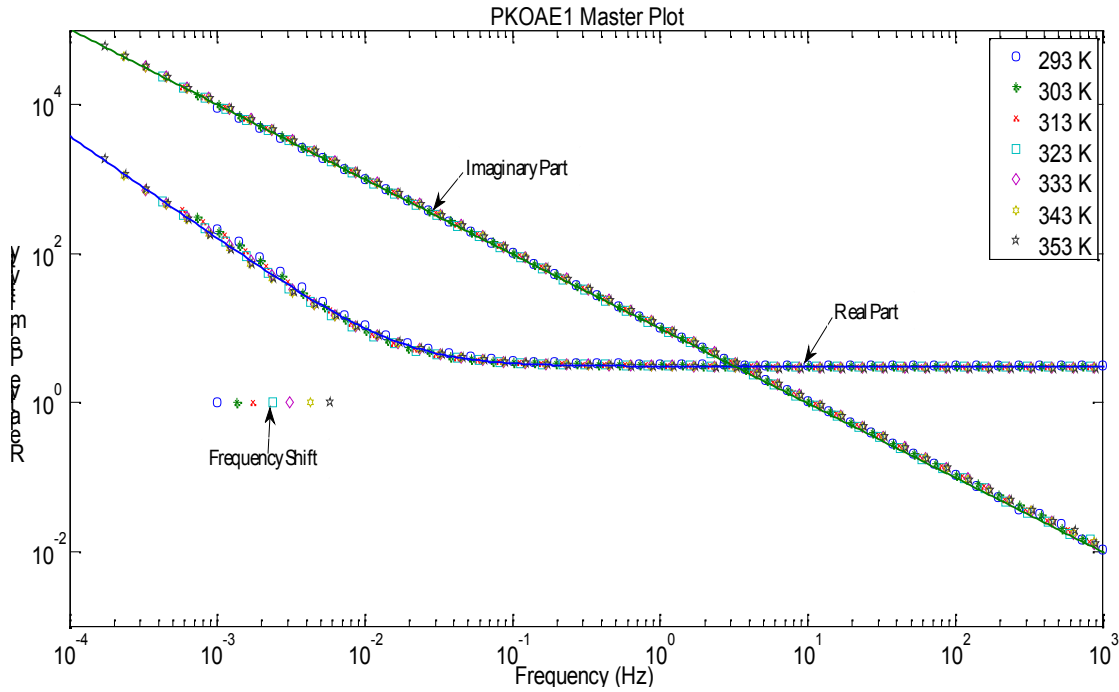


**Fig. 6. Master curve for dielectric response of PKOAE1 (solid line is a trend line)**

The master curve of the alkyl ester samples was constructed by matching the imaginary part of the relative permittivity i.e. the DC conduction component. The low frequency wing of the real part was found not to match with each other, suggesting a different temperature dependent process. PKOAE1 has lower conductance compared with the other ester samples. The conductance increased with processing steps. The charges responsible for conduction in the liquid result from the dissociation of ionic and solid impurities in the liquid. Impurities introduced into the sample during processing may have contributed to the conduction current. At frequencies, below  $10^{-1}$  Hz, the imaginary part maintains a slope of -1, and the real part of the relative permittivity acquires a slope between -1 and -2. This is still an indication of a strong dispersive behaviour (interfacial polarization), an effect arising from the capacitive layer near the electrode.



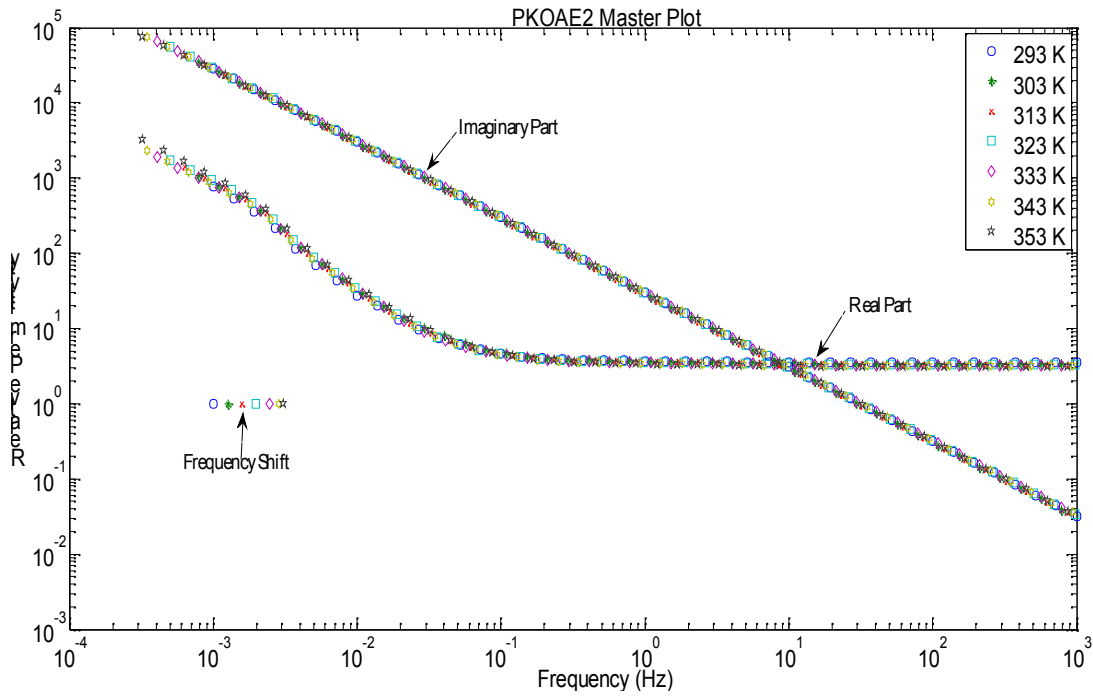


Fig. 7. Master curve for dielectric response of PKOAE2

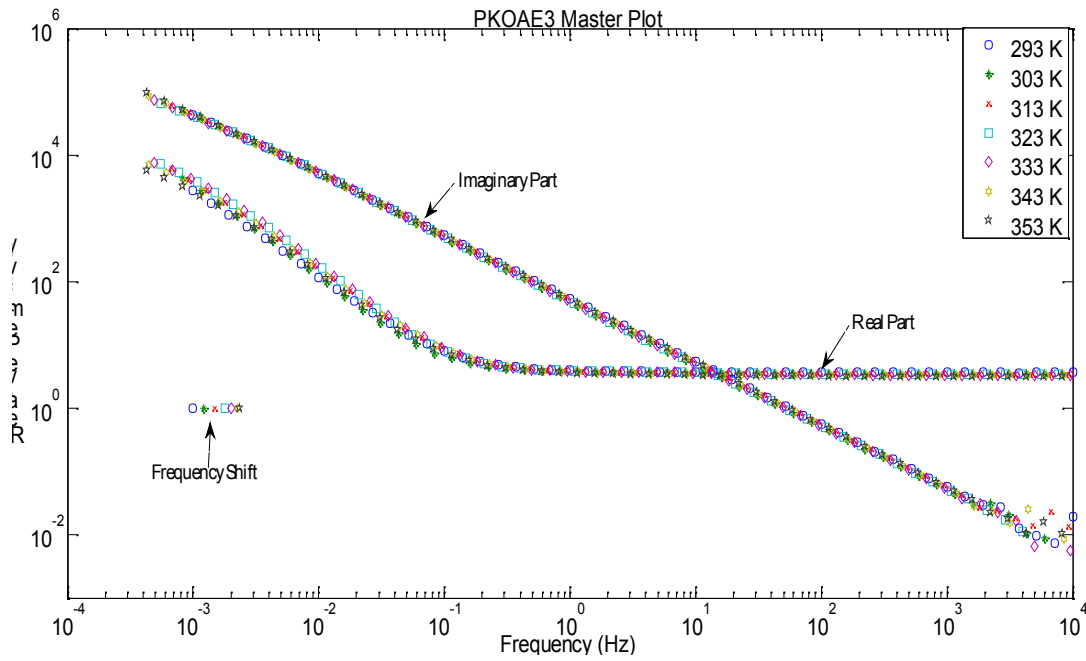
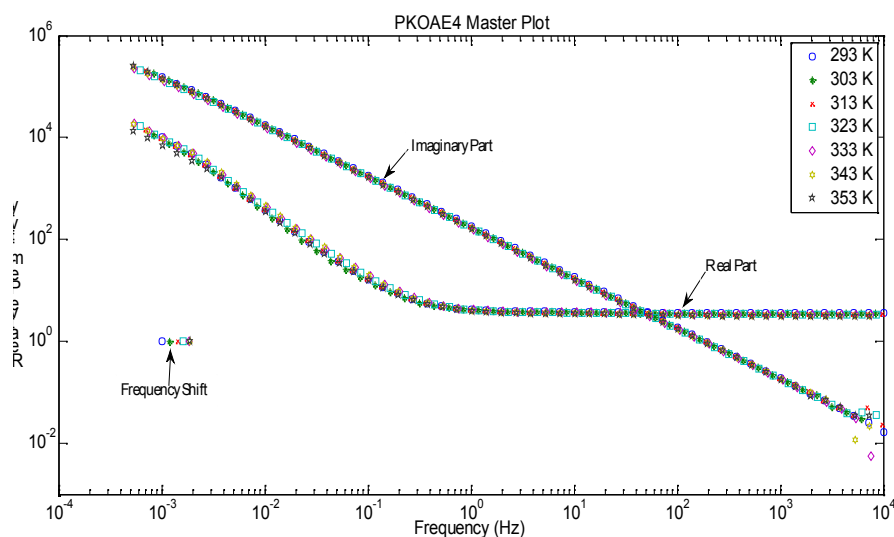


Fig. 8. Master curve for dielectric response of PKOAE3

The ionic species in the fluid drifted to the electrode-liquid interface to accumulate near the electrode surface. Reversal of the applied electric field leads to redistribution of the accumulated charges near the electrode and setting up a new equilibrium. Under constant electric field, a double layer is formed and is thought to be made up of several "layers". In a liquid such as alkyl esters with low conductivity, it is assumed that two layers exist at the electrode [11]. The closest layer to the electrode is referred to as the Stern layer. This is a compact layer of ions next to the electrode. The double layer of the ester samples may have contained the oil molecules and ionic species. Following the Stern layer is a layer of ions that are distributed in a three dimensional region called the diffuse layer. This layer is also referred to as Gouy Chapman layer (Fig. 10). This layer extends into the bulk liquid because of the counter actions of electrostatic field and thermal agitation in the liquid. At higher frequencies, the time scale was too short for the ions to align to form the electric double layer (EDL) at the electrode liquid interface. As the frequency drops below  $10^1$  Hz, the ions have much longer time to align themselves forming the EDL. The formed double layer contributed a finite value that results in increase in the real part of the capacitance.



**Fig. 9. Master curve for dielectric response of PKOAE4**

PKOAE2, PKOAE3 and PKOAE4 appeared to exhibit similar behaviour with PKOAE1. But a close inspection of the spectra reveals that, the real part of dielectric response of the esters undergoes a change below the frequency of  $10^{-1}$  Hz. A very slow response was observed on the real part of the relative permittivity with an approximate slope of -1. The low frequency dispersion is equivalent to a dispersive barrier in series with the bulk conductance. However, the dispersive barrier appeared to have a more complex behaviour compared with the behaviour of PKOAE1 sample within the frequency range studied. At the onset of electrode polarization phenomenon, the frequency dependence of the real relative permittivity is proportional to  $\omega^{n-1}$ , where the value of  $n$  is between 0.45 and 0.65 for the three samples. This slope gradually changes to about -1 at lower frequencies. This suggests that the establishment of the EDL may be tending towards steady state. This change in the low frequency dispersion could be due to the ionic species undergoing interfacial electrochemical processes [4], or ions of lower mobility may have contributed to the EDL formation within the frequency region. Variation in the thickness of the layer at the

electrode-liquid interface may also have caused the change in the slope of the real part of the dielectric response at lower frequencies.

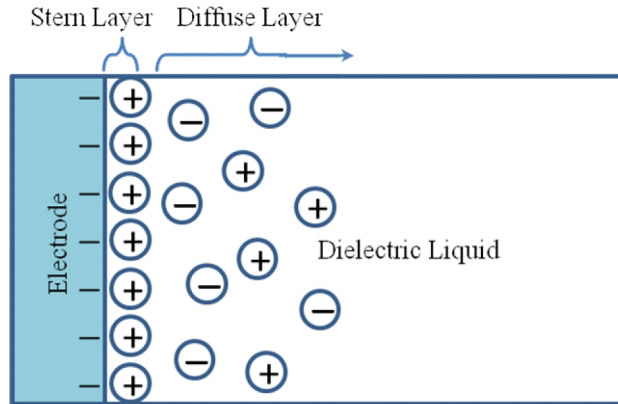


Fig. 10. Model of electric double layer

### 3.3 Arrhenius Behavior of Frequency Response

Information on the influence of thermal energy on the behaviour of the double layer can be extracted from the relaxation frequency. The influence of temperature on the characteristic frequency was determined with equation 3. The plot of the characteristic frequency shift in the dielectric response of PKOAE1, PKOAE2, PKOAE3, and PKOAE4 is shown in Fig. 11.

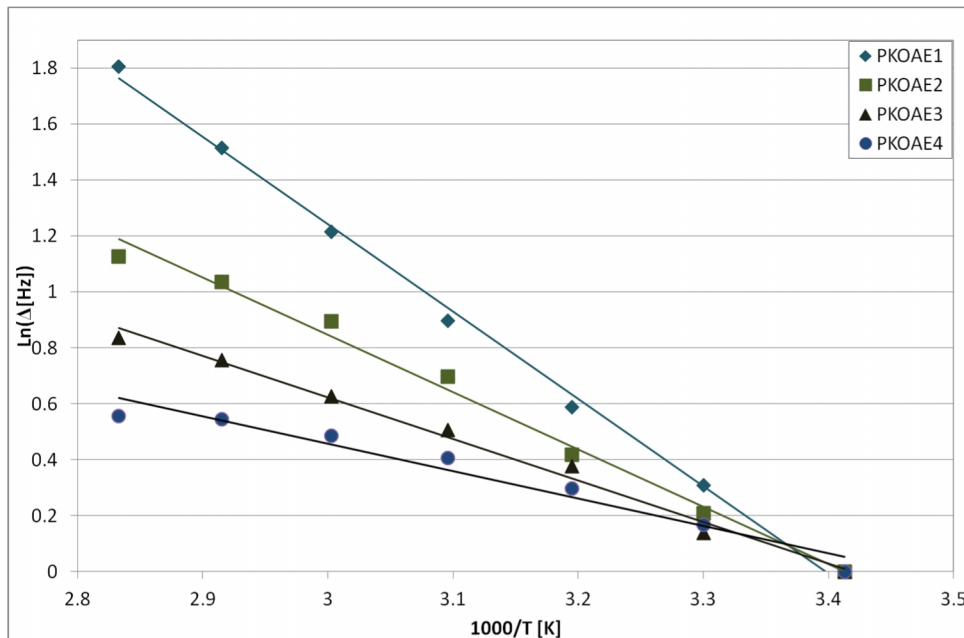
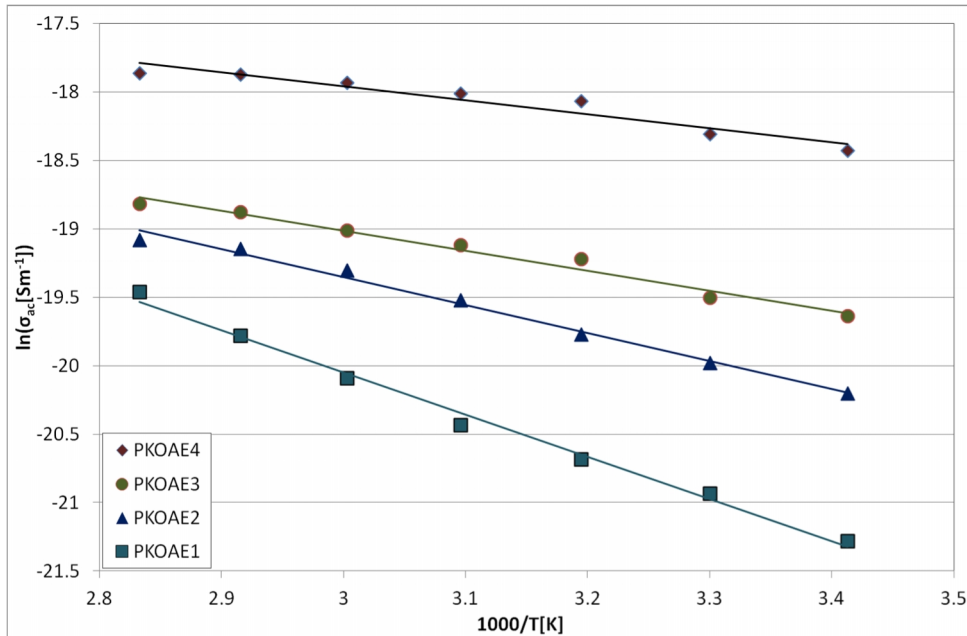


Fig. 11. Characteristic frequency shift of ester dielectric response on Arrhenius axes

The real and imaginary parts of relative permittivity of ester samples obey simple Arrhenius behaviour with correlation coefficients ( $R_2$ ) ranging from 0.96 to 0.99. The ester samples displayed systematic linear shift in the characteristic frequency as the temperature increased. PKOAE1, PKOAE2, PKOAE3, and PKOAE4 possessed activation energies of 0.27, 0.18, 0.13, and 0.08 eV respectively. The single activation energy is an indication that the double layer formation is a thermally activated process. The relaxation time of electrode polarization expressed as [4];

$$\tau_{EP} \propto \frac{1}{T} \exp \frac{c}{kT} \tag{4}$$

decreases with increasing temperature; where  $c$  is a constant for a given liquid. The systematic shift in the relaxation frequency towards higher frequency may be due to changes in the relaxation time of electrode polarization with increasing temperature.



**Fig. 12. Plot of electrical conductivity of ester samples on Arrhenius axes**

Electrical conductivity,  $\sigma_{ac}$  is related to the imaginary part of the relative permittivity,  $\epsilon''$ , with the expression:

$$\sigma_{ac} = \omega \epsilon'' \tag{5}$$

where  $\omega$  is the angular frequency. The AC conductivity of PKOAE1, PKOAE2, PKOAE3 and PKOAE4 calculated using equation 5 is plotted on Arrhenius axes in Fig. 12. The electrical conductivity was evaluated from the imaginary part of the frequency response data of the samples within the temperature range of 20°C to 80°C. The straight lines obtained indicate thermally activated transport mechanisms. The activation energies of PKOAE1, PKOAE2,

PKOAE3 and PKOAE4 derived from this Arrhenius plot are shown in Table 2. The plot of conductivity of the samples calculated from the imaginary part of the dielectric response data shows single activation energies. This suggests that the ionic conduction loss may have been influenced by thermally activated processes. The calculated conductivity increased from PKOAE1 through PKOAE4. The conductivity is relatively constant with frequency as was reported by Bartnikas for most insulating liquids [12].

**Table 2. AC conductivity and activation energy**

Samples	$\sigma_{AC}$ (S/m)	Activation Energy for $\sigma_{AC}$ (eV)
PKOAE1	$5.72 \times 10^{-10}$	0.27
PKOAE2	$1.68 \times 10^{-9}$	0.18
PKOAE3	$2.95 \times 10^{-9}$	0.13
PKOAE4	$9.89 \times 10^{-9}$	0.10

The dielectric response of the synthesized esters has LFD-type interfacial behaviour. The viscosity of the samples increased with processing. The conductivity also increases with processing. Since mobility decreased with increasing viscosity, it follows from the conductivity expressed in equation 5 that an increased concentration of ions may be responsible for the increase in conductivity. This increased concentration may have resulted from impurities formed or introduced during the processing stages.

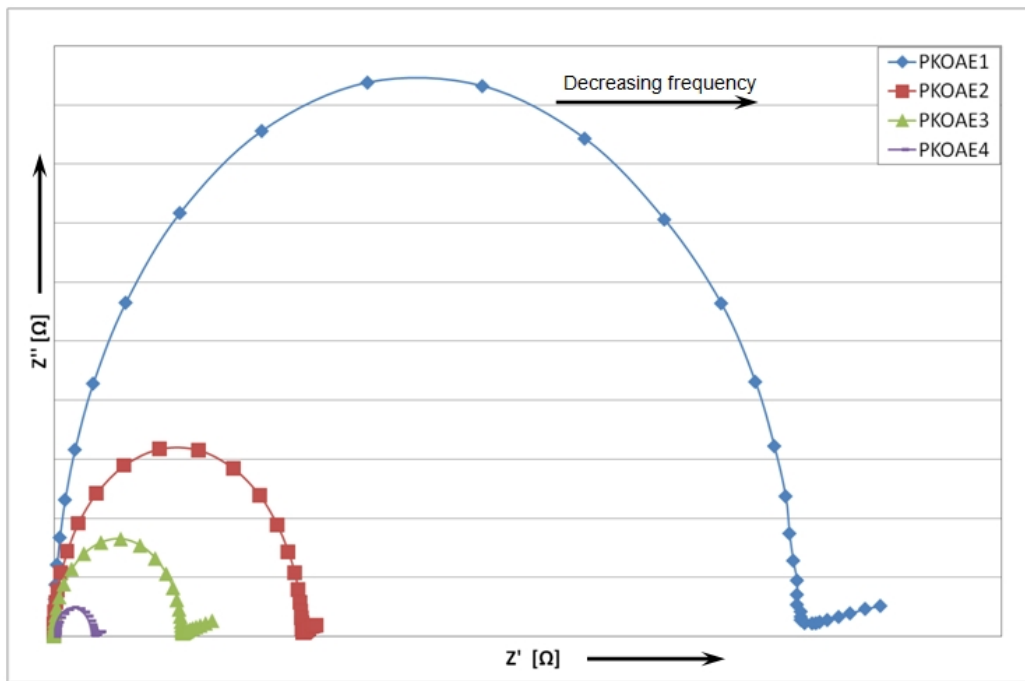


**Fig. 13. Complex plane (Z'' vs Z' plot)**

The dielectric dispersion of the oil increased with temperature due to change in viscosity that accompanied the temperature variation. The decreasing viscosity enhanced the mobility of the charged particles due to the viscosity dependence of mobility of charge carriers in liquids

[12]. This ease in the mobility of more charge carriers results in more mobile charge carriers contributing to the loss phenomena at higher temperatures. The effect leads to a gradual increase in the conductivity of the oil as viscosity decreases.

The dispersive barrier formed in the ester samples appeared to have a complex behaviour. The plot of the response of the ester samples in complex impedance plot is shown in Fig. 13. It clearly displayed a separation of the bulk mechanism from the interfacial phenomenon. The semicircular-like arc which occurs at high frequency region indicates that conductance is the dominant process in the bulk material, while the spurs resulted from the interfacial phenomenon which includes interfacial polarization and a suspected electrochemical or low ionic mobility processes. This means that charge-transfer kinetics alone dictate the conduction process at high frequency region. The area under the semicircular arc reduced as the conductivity of the samples increases. To understand the physical interpretation of the arc, let us consider parallel R-C for the bulk liquid, and the double layer to involve two parallel processes that consists of the double layer capacitance,  $C_n$  and polarization resistance,  $R_n$ . At very high frequency, the contribution of the double layer to the imaginary part of the impedance is zero. As the frequency decreases, the contribution of  $C_n$  becomes finite.  $C_n$  then gives a high reactance and the current passes predominantly through the bulk conductance and polarization resistance. This overall effect is an increasing  $Z'$  and diminishing  $Z''$ . There exists a transition between the semicircular arc and the inclined spur for the respective ester samples. The lowest value for the imaginary part of the impedance corresponds to frequency of  $\tan\delta$  peak. This is the relaxation frequency for electrode polarization ionic species and the corresponding relaxation time can be evaluated from it. The frequency dependence of this region is only from interfacial polarization. At lower frequencies when  $\omega \rightarrow 0$ , the electric double layer becomes dominant and low frequency dispersion as indicated by a low frequency power law, played a significant role in the dielectric response of the material. Interfacial dispersion may be responsible for the nature of the response obtained for the alkyl esters. This response can be represented as a dispersive barrier in series with parallel bulk R-C as shown in Fig. 14. The frequency dependent dispersive barrier may be a set of series combination of polarization resistance,  $R_n$  ( $1/G_n$ ) and capacitance,  $C_n$  connected in parallel as shown in Fig. 14 [13,14].

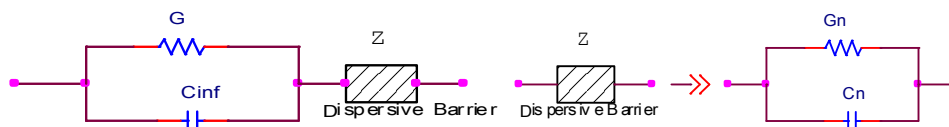


Fig. 14. Equivalent circuit for electrode polarization in alkyl ester

#### 4. CONCLUSION

The dielectric characterization of the synthesized samples was performed over the frequency range  $10^{-3}$  -  $10^6$  Hz and at a number of fixed temperatures. The temperature ranges from  $20^\circ\text{C}$  to  $80^\circ\text{C}$  at an interval of  $10^\circ\text{C}$ . The measurements results presented on master plots enabled the observation of the dielectric responses of the samples down to a frequency of  $10^{-4}$  Hz at  $20^\circ\text{C}$ . Ion transport in the ester samples is a thermally activated process with obtained activation energies that varied between 0.08 eV and 0.27 eV. The activation energy decreased with processing steps. The esters displayed strong low frequency dispersion (LFD). The impurity charge carriers in the fluids influenced the real part of the relative permittivity,  $\epsilon'$  at very low frequencies ( $< 10^{-1}$  Hz). Although the synthesized

esters possessed low viscosity, they have higher conductivity compared with the existing insulating fluids. This may have resulted from an increase in concentration of impurity charges and/or high mobility due to low viscosity.

## **ACKNOWLEDGEMENTS**

I wish to acknowledge Islamic Development Bank for sponsoring this work. The support of National Grid UK is also acknowledged. The contributions of Prof. J.C. Fothergill, City University London, UK, Dr. S.D. Dodd, University of Leicester, UK and Prof Len Dissado, University of Leicester, UK is acknowledged.

## **COMPETING INTERESTS**

Author has declared that no competing interests exist.

## **REFERENCES**

1. Bartnikas R. Alternating-Current Loss and Permittivity Measurements. In: Bartnikas R. Engineering Dielectric, Vol. IIB, Electrical Properties of Solid Materials: Measurement techniques. ASTM Publication. 1987;52-123.
2. Von Hippel AR. Theory. In: Von Hippel A. R. Dielectric Materials and Applications. Massachusetts: The MIT Press. 1954;3-46.
3. Dissado LA, Hill RM. Anomalous low-frequency dispersion. J. Chem. Soc., Faraday Trans. 1984;2(80):291-319.
4. Raju GG. Dielectrics in Electric Fields. Marcel Dekker, Inc; 2003.
5. Jonscher AK. Universal Relaxation Law. London: Chelsea Dielectric Press Ltd; 1996.
6. Abdelmalik AA, Abbott AP, Fothergill JC, Dodd S, Harris RC. Synthesis of a base-stock for electrical insulating fluid based on palm kernel oil. Industrial Crops and Products. 2011;33:532-536.
7. Sharma BK, Liu Z, Adhvaryu A, and Erhan SZ. One-Pot Synthesis of Chemically Modified Vegetable Oils. J. Ag. Food Chem. 2008;56:3049-3056.
8. Abdelmalik AA, Fothergill JC, Dodd SJ. Electrical conduction and dielectric breakdown characteristics of alkyl ester dielectric fluids obtained from palm kernel oil. IEEE Transactions on Dielectrics and Electrical Insulation. 2012;19(5):1623-1632.
9. Carey FA. Organic Chemistry. Fourth Edition, Boston; McGraw Hill Higher Education; 2000.
10. Jonscher AK. Dielectric relaxation in solids. London: Chelsea Dielectric Press; 1983.
11. Schmidt WF. Conduction Mechanism. In: Bartnikas R., Liquids in Engineering Dielectric, Vol. III, Electrical Insulating Liquids. ASTM Publication. 1994;147-260.
12. Bartnikas R. Permittivity and Loss of Insulating Liquid. In: Bartnikas R. Engineering Dielectrics, Vol. III, Electrical Insulating Liquids, ASTM Publication. 1994;3-146.
13. Brett CMA, Brett AMO. Electrochemistry: principles, methods, and applications. Oxford University Press; 1993.

14. Bard AJ, Faulkner LR. Electrochemical methods: fundamentals and applications. 2<sup>nd</sup> edition, John Wiley & Sons, Inc; 2001.

---

© 2014 Abdelmalik; This is an Open Access article distributed under the terms of the Creative Commons Attribution License (<http://creativecommons.org/licenses/by/3.0>), which permits unrestricted use, distribution, and reproduction in any medium, provided the original work is properly cited.

*Peer-review history:*

*The peer review history for this paper can be accessed here:*  
<http://www.sciencedomain.org/review-history.php?iid=299&id=5&aid=2303>